Vortex dynamics and entropic forces in antiferromagnets and antiferromagnetic Potts models

Cristopher Moore,[1,*] Mats G. Nordahl,[2,†] Nelson Minar,[3,‡] and Cosma Rohilla Shalizi[1,4]
[1]*Santa Fe Institute, 1399 Hyde Park Road, Santa Fe, New Mexico 87501*
[2]*Institute of Theoretical Physics, Chalmers University of Technology, S-412 96 Göteborg, Sweden*
[3]*MIT Media Lab, 20 Ames Street, Cambridge, Massachusetts 02139*
[4]*Physics Department, University of Wisconsin, Madison, Wisconsin 53706*
(Received 3 March 1999; revised manuscript received 27 July 1999)

It is well known in models with an interface representation, such as the dimer model, the triangular Ising antiferromagnet, the six-vertex ice model, and the three-state antiferromagnetic Potts model on the square lattice, that topological defects of opposite charge are attracted with an entropically-driven Coulomb force. We examine the Potts model in detail, show explicitly how this force is felt through local fields, and calculate the defects' mobility. We then take two approaches to measuring this force numerically. First, we quench a random initial state to zero temperature and measure the density of defects $\rho(t)$ as a function of time. While this gives some evidence for a local force, we compare it with a free diffusion experiment, and show that the asymptotic decay of $\rho(t)$ depends on the initial distribution of defects rather than the forces between them. Second, we set up initial conditions with a single pair of vortices, and measure the force between them as a function of distance. This gives reasonable agreement with theory, although finite-size effects and a lack of ergodicity play a significant role. [S1063-651X(99)15611-3]

PACS number(s): 05.50.+q, 75.10.Hk, 47.32.Cc, 67.40.Fd

I. INTRODUCTION

A number of models in statistical physics admit an interface representation, such as dimer models [1,2], the triangular Ising antiferromagnet [3,4], the six-vertex ice model [5], and the three-state Potts antiferromagnet on the square lattice. The long-wavelength behavior of the system is then governed by a Gaussian model, with a free energy of the form

$$G = \frac{1}{2} K \int |\nabla h|^2 \, dx \, dy. \tag{1}$$

Here h is the height of the interface and K is a stiffness constant. Thus, there is a free energy cost related to the gradient of the interface.

Topological defects in these models become screw dislocations in this representation, where the topological charge is equal to the Burgers vector B, i.e., the total change in height Δh integrated around the defect. Such a defect has a field around it

$$|\nabla h| = \frac{B}{2\pi r}$$

so the free energy of a defect integrated from a short-distance cutoff r_0 (roughly the lattice spacing) to an interdefect distance r is

$$G = \frac{KB^2}{4\pi} (\log r - \log r_0) \tag{2}$$

just as for dislocations in solids [6]. Integrating this over all space for a pair of defects with Burger vectors B and $-B$ a distance r apart and differentiating with respect to r gives a Coulomb-like attractive force [7]

$$F = -\frac{\partial G}{\partial r} = -\frac{KB^2}{\pi r}. \tag{3}$$

If we are in a viscous regime where F is opposed by frictional forces, we expect F to be proportional to the particles' velocity,

$$\vec{v} = \Gamma F = -\frac{\Gamma K B^2}{\pi r} = \frac{A}{r}, \tag{4}$$

where Γ is the mobility.

Since the energy of a pair of defects is not related to their distance, this force is entirely entropic; that is, two defects are attracted because there are more ways to arrange the surrounding lattice when they are close together. This is explanation enough, but how defects feel this in their local dynamics is somewhat mysterious. In addition, to our knowledge this force has not been measured directly.

We start by reviewing the three-state Potts model on the square lattice and its interface representation. We define a local field and show that the motion of defects under single spin-flip dynamics is in fact correlated with this field, thus justifying Eq. (4) from a microscopic point of view. We also calculate the mobility Γ of the defects.

To confirm the existence of a Coulomb force, we do two kinds of numerical experiments. First, we quench a random initial state to zero temperature and measure the density of defects as a function of time. We find logarithmic corrections to $\rho \propto t^{-1}$ like those seen in the XY model [8]. However, a free diffusion experiment suggests that this occurs whenever

*Electronic address: {moore,shalizi}@santafe.edu
†Electronic address: tfemn@fy.chalmers.se
‡Electronic address: nelson@media.mit.edu

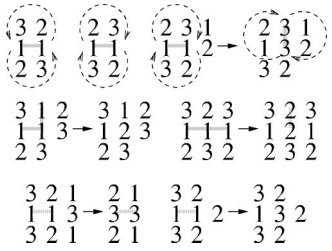

FIG. 1. Counterclockwise and clockwise defects maintain their handedness as they diffuse. Pairs of opposite handedness can annihilate or turn into chargeless excitations, which diffuse until one end is surrounded by only one other color, at which point it can disappear by changing to the third one.

a local conservation law is used to determine the defects' initial positions, whether or not there are forces between them.

Therefore, we also attempt to measure the force directly by placing a pair of defects r apart, allowing the lattice around them to equilibrate, and measuring how they would move toward or away from each other if we allowed them to. We obtain good agreement with a force of the form $\langle \Delta r \rangle = -A/(r+r_0)$, although finite-size effects and a partial lack of ergodicity at $T=0$ affect our results. Using Park and Widom's calculation of the stiffness of the equivalent height model [9] and our calculation of the mobility Γ, we predict that A for the Potts antiferromagnet should be 3/4. This is in reasonable agreement with our results.

II. THREE-STATE POTTS ANTIFERROMAGNET

The q-state antiferromagnetic Potts model is a generalization of the Ising antiferromagnet,

$$U=\sum_{\text{nn}} \delta(s_i,s_j), \tag{5}$$

where each site has a state $s_i \in \{1,2,\ldots,q\}$ and δ is the Kronecker δ function. The states are often thought of as colors, so that the ground state consists of a coloring where no two neighbors have the same color. When $q=3$, this can be thought of as a discretization of the antiferromagnetic XY model,

$$U=\sum_{\text{nn}} \cos(\theta_i-\theta_j), \tag{6}$$

where each site has a unit spin pointing in some direction θ. If the θ_i are restricted to three directions $2\pi/3$ apart, then Eqs. (5) and (6) are equal up to an affine transformation since $\cos(\theta_i-\theta_j)$ depends only on whether θ_i and θ_j are the same or different.

We will focus on this three-state model on the square lattice. Nightingale and Schick [10] showed that it is critical at $T=0$. Baxter [11,12] showed that this is its only phase transition, and solved it there as a hard-squares model. For recent Monte Carlo studies using the Wang-Swendsen-Kotecký cluster algorithm [13], see, e.g., Ferreira and Sokal [14].

Kolafa [15] pointed out that this model supports vortices, as shown in Fig. 1. These change color but preserve their handedness as they diffuse, and two defects of opposite handedness can annihilate when they meet. There are also chargeless excitations, where sites on either side of the ends of the frustrated bond have the same color. These can be annealed away without interacting with other defects, so they disappear exponentially quickly in a quench.

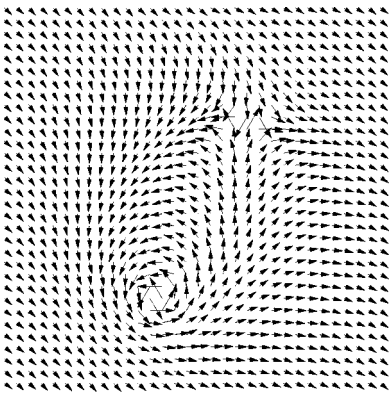

FIG. 2. Local magnetization around a pair of vortices in the $q=3$ Potts antiferromagnet. This picture was obtained by relaxing a 32×32 lattice until only two defects remained, and then holding them fixed for 10^5 updates per site while we averaged the magnetization at each site.

Kolafa defines the charge within a region as a sum around a counterclockwise perimeter,

$$Q=\frac{1}{6}\sum m(s_{i+1}-s_i), \tag{7}$$

where $m(k)=0$, $+1$ or -1, and $m(k)\equiv k \pmod 3$. To translate this into an interface model, define a height function h on the lattice so that $h_i \equiv s_i \pmod 3$, and furthermore h_i

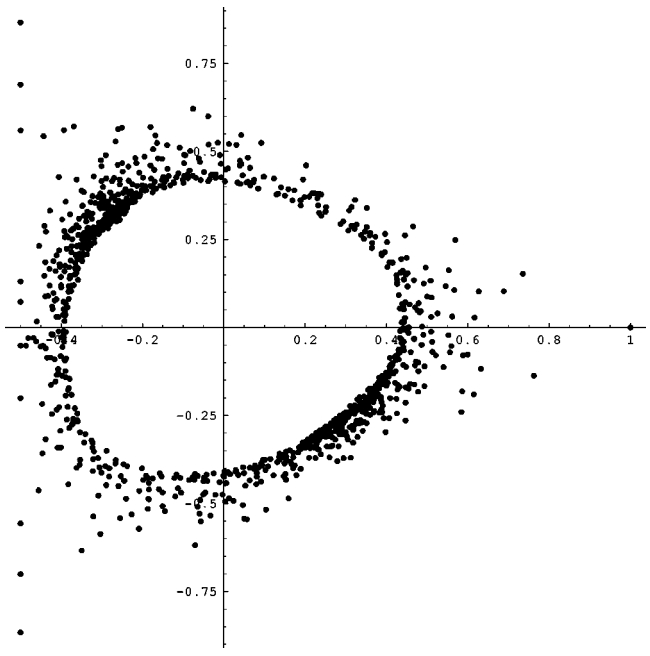

FIG. 3. Scatter plot of the time-averaged local magnetization in Fig. 2.

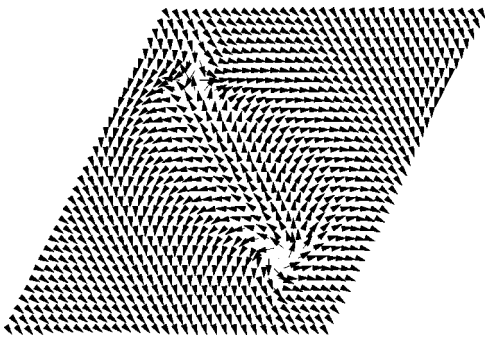

FIG. 4. Picture analogous to Fig. 2 for the triangular Ising antiferromagnet, produced in the same way on a 33×33 rhombic lattice.

$-h_j=\pm1$ between neighboring sites (note we can add a multiple of 3 to h without changing the state). Then Eq. (7) becomes

$$Q=\frac{1}{6}\sum \Delta h,$$

where the sum is around a counterclockwise perimeter. This sum is simply the Burgers vector B, and is ±6 for a single defect. The factor of 1/6 then gives a charge Q of ±1.

Equivalently, we can define a complex local magnetization $\xi_i=(-1)^p e^{2\pi i s_i/3}$, where the three colors correspond to the cube roots of unity, and $(-1)^p$ gives a sign of -1 and $+1$ on odd and even lattice sites, respectively [16]. This makes regions with antiferromagnetic order, say with color 1 on one sublattice and colors 2 and 3 on the other, relatively uniform. Then Q is the winding number of ξ_i around the origin,

$$Q=\frac{1}{2\pi i}\oint \frac{d\xi}{\xi}.$$

In Figs. 2 and 3, we show the time average of ξ for a configuration with two defects. We can clearly see how each vortex produces a field around it which falls off with distance. In Fig. 4 we show a similar picture for the triangular Ising antiferromagnet, with a local magnetization defined as in [17].

We will now explore how defects could feel a Coulomb force under single spin-flip dynamics, where at each step we choose a random site in the lattice and change its color unless this would increase the energy. If we define a field $\vec{E}$ perpendicular to each bond so that the higher color in the cyclic ordering $3>2>1>3$ is on its left, then $\vec{E}$ will tend to point towards negative (clockwise) defects and away from positive (counterclockwise) ones. Note that $\vec{E}$ is simply $\vec{\nabla}h$ rotated by 90°.

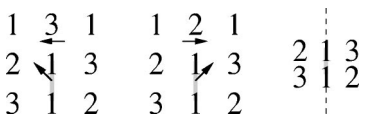

FIG. 5. If we define a field $\vec{E}$ on each bond so that the higher color in the cyclic ordering is on its left, the movement of a positive defect is proportional to $\vec{E}$ averaged over the two dashed edges.

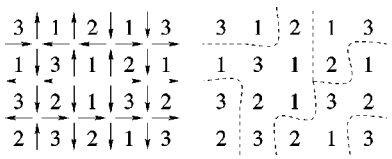

FIG. 6. Mapping the $q=3$ Potts antiferromagnet onto the six-vertex ice model and the loop-covering model. In the former, the defect corresponds to a monopole, an undefined edge with six arrows emerging from it.

As Fig. 5 shows, if we flip one site of a positive defect, the displacement of its midpoint from that site is just one-half the field on the edge extending the frustrated bond. Since both sites are equally likely, the average movement of the defect's midpoint is proportional to $\vec{E}$ averaged over the two bonds extending from the defect,

$$\langle\Delta\vec{x}\rangle=\frac{1}{4}\sum \vec{E}.$$

If we define a discrete contour integral around a boundary with bonds $\vec{b}$, we can rewrite Kolafa's formula as

$$Q=\frac{1}{6}\sum_{\vec{b}} \vec{E}\times\vec{b},$$

so if $\vec{E}$ is sufficiently uncorrelated around a large perimeter, we have

$$E=\frac{6Q}{2\pi r}=\frac{B}{2\pi r}.$$

If we make a local mean-field approximation in which the $\vec{E}$ is uncorrelated between the two dashed edges, so that $(1/2)\Sigma\vec{E}=\vec{E}$, then defects of charge Q and Q' are affected by a $1/r$ force,

$$\langle\Delta\vec{x}\rangle=\frac{3QQ'}{2\pi r}.$$

The constant here is only approximate, since the two dashed edges are not uncorrelated. Similar arguments can be made for the triangular antiferromagnet, the six-vertex ice model, and a related Villain model [18].

Lenard [19] pointed out that orienting the bonds of the dual lattice according to $\vec{E}$ maps the $q=3$ square Potts antiferromagnet onto the six-vertex ice model, giving both models the ground-state entropy of $\frac{3}{2}\log\frac{4}{3}$ per site calculated by Lieb [20]. When defects are present, this mapping breaks down as shown in Fig. 6. The frustrated bond has three outgoing or incoming arrows at each end. Thus defects act like monopoles composed of a bound pair of vertices with an unoriented bond between them. Nijs *et al.* [21] defined a 27-vertex model that includes bonds and vertices of this type and studied its scaling properties. We note that the Potts model can also be thought of as a fully packed loop model, in which every vertex is covered by exactly one loop [22].

III. ENTROPIC FORCES ON A DISCRETE LATTICE

We saw in the Introduction how the interface model, and the Gaussian approximation to it we assume holds in the long-wavelength limit, give us an entropy-driven free energy gradient ΔG proportional to $\log r$ and therefore a Coulomb force between defects. However, it is instructive to look directly at the Potts model and examine how such an entropy gradient could arise on a discrete lattice. The interface model is not the only way to derive this; for the dimer model on the square lattice, for instance, Fisher and Stephenson [23] used Pfaffians and Toeplitz determinants to show that the number of configurations with two ''holes'' a distance r apart is reduced by $Ar^{-1/2}$, so $\Delta G=(1/2)\log r$. Ioffe and Larkin [24] pointed out that this leads to a Coulomb force. In addition, Zeng and Leath [25] performed numerical calculations of the cost of dislocation pairs in a randomly pinned fully packed loop model, and found a cost proportional to $\log r$.

One simple counting argument goes as follows. Suppose we are trying to extend a spin configuration outward from a square region of the lattice by adding an additional layer of l sites around its perimeter. For the Potts model, successive sites have colors s_i differing by ± 1, and the sum in Eq. (7) is the total displacement of a walk of length l. The number of such walks is

$$\binom{l}{l/2-6Q},$$

where Q is the charge inside the perimeter. The larger Q is, the greater the constraint on the walks, and the lower the entropy will be. If we ignore the interaction between successive layers, which of course we cannot, then the entropy of the set of states surrounding a charge Q (we take Boltzmann's constant to be 1) is

$$\begin{aligned} S_Q &\approx \ln \prod_{l=0}^{r} \binom{l}{l/2-6Q} = \sum_{l=0}^{r} \ln \binom{l}{l/2-6Q} \\ &= S_0 - \sum_{l=0}^{r} \left[\ln \binom{l}{l/2} - \ln \binom{l}{l/2-6Q} \right] \\ &\approx S_0 - (6Q)^2 \sum_{l=0}^{r} \frac{1}{l} \approx S_0 - A\,Q^2 \ln r \end{aligned}$$

for some constant A. We cut off our sum at some maximum perimeter proportional to the interdefect distance r, outside which the charge Q is presumably canceled by defects of the opposite type.

While the assumption of independent layers is hugely wrong (for instance, it gives a ground state entropy per site of $s_0=S_0/N=2$) we find that the presence of a charge Q reduces the entropy by an amount $-\Delta S$ proportional to $Q^2 \ln r$. We can think of this as a contribution to an effective free energy,

$$G=-\Delta S=A\,Q^2 \ln r$$

reproducing the form of Eq. (2).

As another approach, Kotecký [26] pointed out that the entropy of the Potts model can be related to the energy of a ferromagnetic Ising model at a nonzero effective temperature, since the entropy of one sublattice is higher if sites on the other sublattice are the same. An odd site (say) has two choices of color if its four neighbors have the same color, or equivalently if the field $\vec{E}$ points clockwise or counterclockwise around all four bonds, and only one choice otherwise. Recall that the field $\vec{E}$ determines whether the color changes by $+1$ or -1 between neighbors. If we define the probability of the color increasing in the x and y directions as p_x and p_y, respectively, we have

$$p_x=(1-E_y)/2,$$

$$p_y=(1+E_x)/2,$$

where E_x and E_y are the components of the average field. If $\vec{E}$ is slowly varying, and if the colors of the four neighbors are independent, which they are not, the probability of all four having the same color is

$$2p_x(1-p_x)p_y(1-p_y)=\frac{1}{8}(1-E_x^2)(1-E_y)^2 \approx \frac{1}{8}(1-E^2)$$

for small fields $E \ll 1$. The average entropy per site is

$$s=\frac{\ln 2}{8}(1-E^2)=s_0-\frac{\ln 2}{8}E^2,$$

where s_0 is a (badly underestimated) ground state entropy of $(1/8)\ln 2$ per site. The effective free energy is then increased by

$$G=-\Delta S=\frac{\ln 2}{8}\int E^2\,dx\,dy, \tag{8}$$

giving an energy density proportional to the square of the field, just as in electromagnetism. Since this field is simply ∇h rotated by 90°, this again justifies the Gaussian model of Eq. (1).

IV. VISCOUS FORCES AND MOBILITY

To show how an entropy gradient can drive a first-order force, suppose that we group the set of spin configurations with two defects into a set of macrostates $\Sigma(r)$, one for each interdefect distance r. As the defects move towards and away from each other, we can describe the system as a biased random walk

$$\cdots \rightleftarrows \Sigma(r-1) \rightleftarrows \Sigma(r) \rightleftarrows \Sigma(r+1) \rightleftarrows \cdots.$$

If we assume that this walk is a Markov process that has not yet had time to hit the absorbing state $\Sigma(0)$ where the defects annihilate, and if during this transient all microstates with two defects are equally likely, then the ratio of transition probabilities between neighboring macrostates must be the ratio of the number of microstates in them,

$$\frac{P(r \to r+1)}{P(r+1 \to r)}=\frac{\Omega(r+1)}{\Omega(r)},$$

where $\Omega(r)$ is the number of microstates with defects r apart. The average motion is then

$$\langle \Delta r \rangle = P(r \to r+1) - P(r+1 \to r) = 2\Gamma \frac{\Omega(r+1) - \Omega(r)}{\Omega(r+1) + \Omega(r)}$$

$$\approx \Gamma \frac{1}{\Omega} \frac{\partial \Omega(r)}{\partial r} = \Gamma \vec{F},$$

where

$$\Gamma = (1/2)[P(r \to r+1) + P(r+1 \to r)] \tag{9}$$

can be thought of as a mobility, and

$$\vec{F} = \frac{\partial S(r)}{\partial r} = -\frac{\partial G}{\partial r}$$

is the entropic force where $S = \log \Omega$.

To calculate Γ for the Potts antiferromagnet, we need to take into account the fact that a diffusing defect alternates between horizontal and vertical bonds. If we assume for simplicity that $\vec{E}$ is in the x direction, a vertical defect which flips to a neighboring horizontal bond has an equal probability of flipping back to its original position or moving to the vertical bond one site away. If $P_{\rightarrow}$ and $P_{\leftarrow}$ are the probabilities that it will move to the horizontal bond to its right and left, respectively, after two time steps we have $P(r \to r+1) = P_{\rightarrow}/2$ and $P(r+1 \to r) = P_{\leftarrow}/2$. Since $P_{\rightarrow} + P_{\leftarrow} = 1$, plugging these into Eq. (9) and dividing by 2 since Γ is inversely proportional to time gives $\Gamma = 1/8$.

We can then calculate the coefficient $A = \Gamma K B^2/\pi$ of Eq. (4) exactly. Park and Widom [9], using the exact solution of the six-vertex ice model, showed that the free energy of an interface of width L across a height difference of $\Delta h = \pm 2$ is $2\pi/6L$, and Burton and Henley [27] point out that setting this equal to $(1/2)K(\Delta h/L)^2 L$ gives $K = \pi/6$.

Combining these values of Γ and K with the Burgers vector $B = 6$ gives $A = 3/4$. We will compare this to our numerical measurements below.

V. RELAXATION AND DIRECT MEASUREMENTS OF THE FORCE

One way to detect a force between defects would be to start the system in a random initial state and allow it to relax. If defects of opposite charge are attracted, they would be expected to meet and annihilate each other more quickly than they would by random diffusion. Yurke *et al.* [8] discuss the relaxation dynamics of the XY model, in which vortices of opposite type are attracted with a Coulomb force. Assuming a viscous dynamics $\vec{v} = \Gamma \vec{F}$ where the mobility Γ is inversely proportional to $\log r$, they use simple scaling arguments to show that the defect density ρ obeys

$$\frac{1}{\rho^2} \frac{d\rho}{dt} = \frac{C}{\log(\rho/\rho_c)}, \tag{10}$$

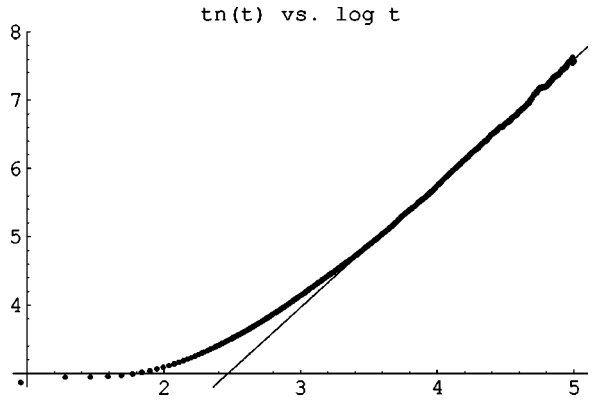

FIG. 7. Plot of $tn(t)$ vs $\log_{10} t$ for the triangular antiferromagnet. The straight line suggests that $n(t) \propto (\log t)/t$ for large t, and extends about a decade and a half. The data were taken by averaging 100 trials of 10^5 updates per site on a 4096×4096 lattice, at which time ~ 75 defects remained. The y axis is in units of 10^6 particles times time.

where ρ_c is a core density and C is a constant. Note that the left-hand side of Eq. (10) is constant for the mean-field behavior $\rho \propto t^{-1}$. The leading behavior of ρ as a function of time is then

$$\rho \propto \frac{\log t}{t} + O\left(\frac{\log \log t}{t}\right)$$

modifying the asymptotic behavior $\rho \propto t^{-1}$ with a logarithmic correction. They confirm the existence of this correction through numerical experiments.

We have performed similar experiments for the Potts model, the triangular antiferromagnet, and a Villain model related to the ice model [18]. In each case, we quenched the system from $T = \infty$ (a random initial state) to $T = 0$, and measured the number of defects $n(t)$ as a function of time. In Fig. 7 we graph $tn(t)$ against $\log t$ for the triangular antiferromagnet, averaged over 100 runs of 10^5 updates per site each on a 4096×4096 lattice. While logarithmic corrections are difficult to establish numerically, $n(t)$ seems to behave as $(\log t)/t$ over one and a half decades in t. In addition, in Fig. 8 we use the same data to graph $\rho^2 (d\rho/dt)^{-1}$ and fit it to

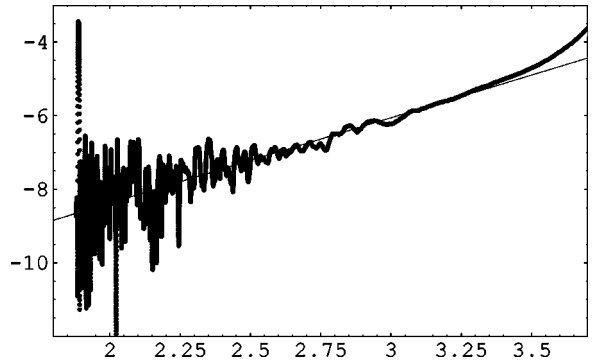

FIG. 8. Plot of $\rho^2 (d\rho/dt)^{-1}$ vs $\log_{10} \rho$ for the triangular antiferromagnet, using the same data as in Fig. 7. The derivative at each time t was defined by a linear fit to 101 data points centered around t. The fit is to the form in Eq. (10). If the mean-field behavior $\rho \propto t^{-1}$ held, the graph would be a horizontal line. The y axis is in units of 10^6 particles times time.

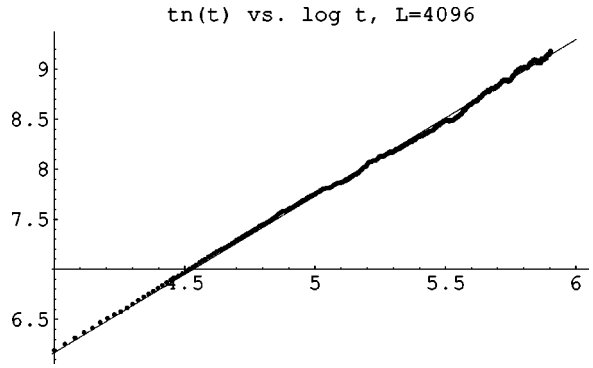

FIG. 9. Plot of $tn(t)$ vs $\log_{10} t$ in a continuous-time free diffusion experiment, where the triangular antiferromagnet was used to set up the initial distribution of defects. The straight line suggests that $n(t) \propto (\log t)/t$, and extends three decades. The data were taken by averaging 100 trials of 8×10^5 updates per site each on a 4096 $\times$4096 lattice until $\sim$100 defects remained. The y axis is in units of 10^7 particles times time.

$C^{-1}\log(\rho/\rho_c)$, as per Eq. (10). We obtain a good fit over a decade and half in ρ, with a core density $\rho_c = 0.02$. Results from the other two models are similar.

However, this turns out not to be a good test for a Coulomb force. We have performed a continuous-time free diffusion experiment, in which we use a random state of the triangular antiferromagnet to set up the initial distribution of defects. We then diffuse the defects with random walks, moving them up, down, left, and right with equal probability, and annihilate pairs of opposite charge when they meet. Thus, the defects have the same initial distribution and correlations as in the antiferromagnet, but no forces between them.

Since these systems obey a Gauss-like law as in Eq. (7), the total charge in a region of size l is a sum of $O(l)$ surface terms, rather an extensive sum of $O(l^2)$ random variables. Thus the total charge fluctuates as $O(l^{1/2})$ rather than $O(l)$, and defects of opposite charge are well mixed with each other in the initial condition, giving a decay close to the mean-field behavior $\rho(t) \propto t^{-1}$. With uncorrelated initial conditions, defects of like type clump into domains, giving a $t^{-1/2}$ decay [28,29].

In Fig. 9 we graph $tn(t)$ for a 4096$\times$4096 lattice over a continuous time of 8×10^5 updates per site. The data appears to have the same asymptotic behavior of $(\log t)/t$, and fits of $\rho^2(d\rho/dt)^{-1}$ to $\log\rho$ are at least as convincing as for the models we studied. In other words, the asymptotic behavior of ρ is more a consequence of the correlations in the defects' initial positions than of the forces between them. This is presumably because a $1/r$ force causes the length scale of the system to grow asymptotically as $t^{1/2}$, no faster than diffusion would anyway. At short times, however, ρ decreases faster in these models than in the free diffusion experiment, indicating that attractive forces play a role early on when defects are relatively close together.

Even if the behavior of ρ at long times does not confirm the existence of a Coulomb force, we can argue that it does show that the force between defects does not fall off more slowly than $1/r$. Generalizing the argument of [8], if the force between two defects goes as $r^{-\alpha}$ for some $\alpha<1$ and the mobility is roughly constant, the typical velocity is

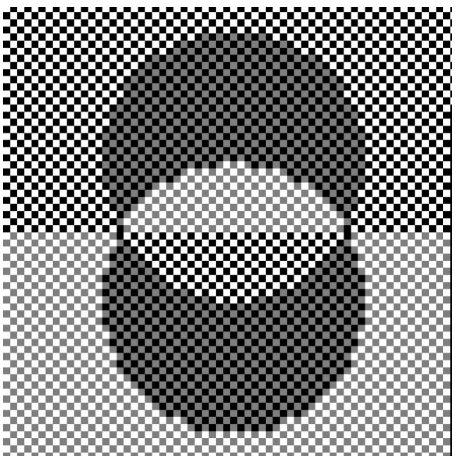

FIG. 10. Initial condition with two vertical defects an even distance away from each other. The six checkerboard phases cycle around the defects, meeting at angles of $\pi/3$.

$$\frac{d\xi}{dt} \propto \xi^{-\alpha},$$

where ξ is the length scale of the system. Then $\xi \propto t^{1/(1+\alpha)}$, and the defect density is

$$\rho \propto \xi^{-2} \propto t^{-2/(1+\alpha)}.$$

If $\alpha<1$, then ρ would decay faster than t^{-1}. Since we do not observe this, we claim that the ''field lines'' of this force spread out, and are not concentrated between defects. (In another paper, in progress, we argue that field lines do bunch into tubes when a ferromagnetic next-nearest-neighbor interaction is added.)

In the case of the $q=3$ square Potts antiferromagnet, we have also measured the force between defects directly. In an effort to sample the set of configurations with two defects a particular distance away from each other, we set up an initial condition with two vertical defects of opposite type as in Fig. 10, and then let the lattice evolve while keeping these defects fixed. We did this on lattice sizes of 32, 64, 128, and 256, averaging over 10^7 updates per site in each case after an initial equilibration of 10^3 updates per site. Letting the inter-defect distance range up to 1/3 the lattice size, we perform a least-squares fit to the form

$$\langle \Delta r \rangle = -\frac{A}{r + r_0},$$

where r_0 is a core radius. This fit seems to work fairly well.

Our values for A and r_0 for various lattice sizes L are

L	A	r_0
32	1.142	2.573
64	0.978	1.956
128	0.906	1.652
256	0.869	1.494

These show considerable finite-size effects. Since the model is critical at $T=0$, we assume that A converges to its exact value as a power law in the lattice size. A least-squares fit to the form $A(L) = A + CL^{-\alpha}$ gives an exponent of $\alpha = 1.137$ and an extrapolated value of $A = 0.843$. This is much larger

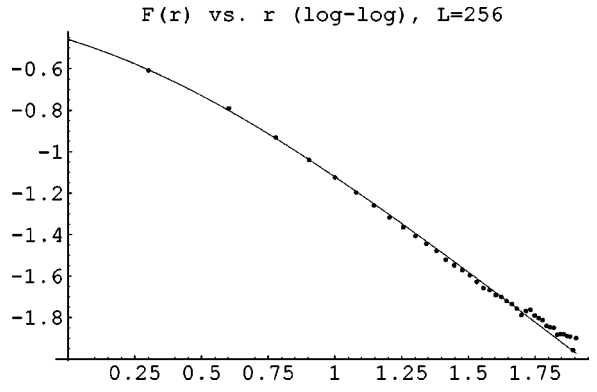

FIG. 11. Force between two defects as a function of their distance r, This data were obtained on a lattice of size 256 by starting with the initial condition shown in Fig. 10 and averaging the force over 10^7 updates per site after an initial equilibration of 10^3 updates per site. During these updates, the defects are kept fixed, and $\langle \Delta r \rangle$ is defined according to which way they would move if we allowed them to. The form $A/(r+r_0)$ fits the data within the expected error over most of the range.

than the local mean-field approximation $3/2\pi \approx 0.477$ given in Sec. II. However, it differs by only 12% with the value of 3/4 derived from the exact solution of the Potts model and our calculation of the mobility in Sec. IV. Since this extrapolation is based on only four different lattice sizes, it should be easy to improve this agreement with further numerical work.

We suspect that A is larger on smaller lattices because field lines have less room to spread out. We would like to analyze this in terms of image charges, but it is somewhat unclear how to do this. In fact, even when the interdefect distance is half the lattice size, our prediction of $A/(r+r_0)$ for the force is only 25% off, even though by symmetry the image charges should cancel and make the force zero. The reason for this is that single spin-flip dynamics is not quite ergodic at zero temperature when the defects are held fixed; the boundaries between checkerboard domains in Fig. 11 can move and join with droplet boundaries, but not cross. Therefore, the topology of the field lines stays the same, with five connecting the defects directly and only one going around the lattice the other way. In a sense, this may be a happy accident, allowing us to observe the force at larger distances than we would be able to on finite lattices if image charges were fully felt. It also means that the measured value of A may depend on the topology of the initial condition; however, experiments on lattices of size 64 and 128 where all six field lines connect the two defects directly give values of A and r_0 differing from those above by less than 0.4%, so topology may in fact not matter that much.

We also tried to use the Wang-Swendsen-Kotecký cluster algorithm [13] to sample the set of configurations with a pair of defects at particular places. Unfortunately, while cluster-flipping moves leave defects in the same place, they sometimes replace two defects of opposite charge with two chargeless ones. Finding an algorithm more efficient than single spin-flip dynamics to sample the set of two-defect configurations would seem to be an open question.

VI. CONCLUSION

We have examined topological defects or vortices in the three-state Potts antiferromagnet on the square lattice. Both the height representation and arguments on the discrete lattice suggest that positive and negative defects are attracted by an entropically driven Coulomb force. We have confirmed this through numerical experiments, and obtained reasonable agreement between the magnitude of this force and its theoretical value, derived from the exact solution of the Potts model and our calculation of the defects' mobility.

Both this model [30] and the triangular Ising antiferromagnet [31,4] are known to have Kosterlitz-Thouless-like phase transitions [32] in the same universality class as the six-state clock model [33,34] when a ferromagnetic next-nearest-neighbor interaction is added. In another paper, we hope to look at how this interaction, and the screening effect of particle-antiparticle pairs at nonzero temperatures, affects the forces between defects. Finally, we note that Bakaev and Kabanovich [35] have discussed the motion of a different kind of defect in the $q=3$ Potts antiferromagnet, a hole with an undefined color.

ACKNOWLEDGMENTS

C.M. is grateful to Mark Newman, Chris Henley, Chen Zeng, Roman Kotecký, Michael Lachmann, and Andrew Pargellis for helpful discussions; N.M. thanks the National Science Foundation Research Experience for Undergraduates Program.

[1] W. Zheng and S. Sachdev, Phys. Rev. B **40**, 2704 (1989).
[2] L. S. Levitov, Phys. Rev. Lett. **64**, 92 (1990).
[3] H. W. J. Blöte and H. J. Hilhorst, J. Phys. A **15**, L631 (1982).
[4] B. Nienhuis, H. J. Hilhorst, and H. W. J. Blöte, J. Phys. A **17**, 3559 (1984).
[5] H. van Beijeren, Phys. Rev. Lett. **38**, 993 (1977).
[6] J. Friedel, *Dislocations* (Pergamon, Oxford, 1964).
[7] M. Peach and J. S. Koehler, Phys. Rev. **80**, 436 (1950).
[8] B. Yurke, A. N. Pargellis, T. Kovacs, and D. A. Huse, Phys. Rev. E **47**, 1525 (1993).
[9] H. Park and M. Widom, Phys. Rev. Lett. **63**, 1193 (1989).
[10] M. P. Nightingale and M. Schick, J. Phys. A **15**, L39 (1982).
[11] R. J. Baxter, Proc. R. Soc. London, Ser. A **383**, 43 (1982).
[12] R. J. Baxter, J. Math. Phys. **11**, 3316 (1970).
[13] J.-S. Wang, R. H. Swendsen, and R. Kotecký, Phys. Rev. Lett. **63**, 109 (1989); Phys. Rev. B **42**, 2465 (1990).
[14] S. J. Ferreira and A. D. Sokal, e-print cond-mat/9811345.
[15] J. Kolafa, J. Phys. A **17**, L777 (1984).
[16] J. L. Cardy, Phys. Rev. B **24**, 5128 (1981).
[17] S. Fujiki, K. Shutoh, and S. Katsura, J. Phys. Soc. Jpn. **53**, 1371 (1984).
[18] C. Moore, M. G. Nordahl, N. Minar, and C. Shalizi, e-print cond-mat/9902200.
[19] A. Lenard (unpublished).
[20] E. H. Lieb, Phys. Rev. **162**, 162 (1967).
[21] M. P. M. Nijs, M. P. Nightingale, and M. Schick, Phys. Rev. B

26, 2490 (1982).
[22] G. T. Barkema and M. E. J. Newman, Phys. Rev. E **57**, 1155 (1998).
[23] M. E. Fisher and J. Stephenson, Phys. Rev. **132**, 1411 (1963).
[24] L. B. Ioffe and A. I. Larkin, Phys. Rev. B **40**, 6941 (1989).
[25] C. Zeng and P. L. Leath, e-print cond-mat/9810154; C. Zeng, P. L. Leath, and D. S. Fisher, e-print cond-mat/9807281.
[26] R. Kotecký, Phys. Rev. B **31**, 3088 (1985).
[27] J. K. Burton, Jr. and C. L. Henley, J. Phys. A **30**, 8385 (1997).
[28] D. Toussaint and F. Wilczek, J. Chem. Phys. **78**, 2642 (1983).
[29] M. Bramson and J. L. Lebowitz, J. Stat. Phys. **62**, 297 (1991).
[30] I. Ono, J. Phys. Soc. Jpn. **53**, 4102 (1984); Suppl. Prog. Theor. Phys. **87**, 102 (1986).
[31] D. P. Landau, Phys. Rev. B **27**, 5604 (1983).
[32] J. M. Kosterlitz and D. J. Thouless, J. Phys. C **6**, 1181 (1973).
[33] J. V. José, L. P. Kadanoff, S. Kirkpatrick, and D. R. Nelson, Phys. Rev. B **16**, 1217 (1977).
[34] A. Yamagata and I. Ono, J. Phys. A **24**, 265 (1991).
[35] A. V. Bakaev and V. I. Kabanovich, Mod. Phys. Lett. B **11**, 293 (1997).